Available online at www.sciencedirect.com
SCIENCE DIRECT
Cement and Concrete Research 35 (2005) 344–350
CEMENT AND CONCRETE RESEARCH

Approximate migration coefficient of percolated interfacial transition zone by using the accelerated chloride migration test

C.C. Yang[a,*], S.W. Cho[b]

[a]Institute of Materials Engineering, National Taiwan Ocean University, 2 Pei-Ning Road, Keelung 202, Taiwan, ROC
[b]Department of Building Engineering and Architecture, China Institute of Technology, Taipei, Taiwan, ROC

Received 8 December 2003; accepted 24 May 2004

Abstract

In this study, the electrochemical technique is applied to accelerate chloride ion migration in cement-based material to estimate its migration coefficient. In order to investigate the chloride migration coefficient of percolated interfacial transition zone (ITZ) on the chloride migration coefficient of specimen, specimens with cylindrical aggregates of the same height as the specimen were cast and tested. In this study, the volume fraction of aggregate is constant and the varied lateral surface area of the aggregate cylinder was obtained by using different diameters and number of aggregate. The chloride migration coefficient of cement-based material was determined experimentally as a function of the lateral surface area of aggregate. A model obtained for the migration coefficient of cement-based material and the regression analysis are used to determine the approximate chloride migration coefficient of the percolated ITZ. Based on the experimental and regression analytical results, the approximate percolated ITZ migration coefficient is 40.6, 35.5, and 37.8 times of the altered migration coefficient of matrix mortar for the water/cement (w/c) ratio of 0.35, 0.45, and 0.55, respectively.

Keywords: Interfacial transition zone; Transport properties; Durability; Chloride; Electrochemical properties

1. Introduction

In normal concrete or mortar, the hydrated matrix surrounding the aggregate has different microstructures resulting from the water/cement (w/c) ratio gradient developed at the near-aggregate surface region [1]. This layer around the aggregate is called the interfacial transition zone (ITZ), which is characterized by a higher concentration of calcium hydroxide crystals and an increased porosity relative to the matrix paste [2–7]. Many researchers have analyzed the microstructure of ITZ in cement-based materials by the use of scanning electron microscopy (SEM) [8–11], energy dispersion X-ray spectrometry (EDX) [12], backscattered electron (BSE) imaging [3–6,11,13], and mercury intrusion porosimetry (MIP) [14,15].

Based on MIP experimental data and on the analysis of a 3D mortar model, the maximum porosity of ITZ is about three times higher than the matrix paste [16]. Using the migration test and regression analysis results, the approximate chloride migration coefficient of ITZ is 2.83 times greater than that of the matrix for the ITZ thickness is assumed as 20 μm [17]. Researchers at National Institute of Standards and Technology (NIST) have developed numerical models describing the microstructure of cement-based materials using digital image analysis techniques [18,19]. The models have applied to determine electrical conductivity of ITZ [20]. Using the results of Winslow et al. [15], Shane et al. [20] pointed out that the ITZ has become percolated between the sand volume fractions of 0.45 and 0.49.

Shah [21] and Delagrave et al. [22] pointed out that the inclusion of aggregates in the hydrated cement past matrix has two opposite effects on the transport properties. The dilution and tortuosity effects reduce concrete permeability while the ITZ and percolation effects increase permeability.

In this study, the chloride migration coefficient of cement-based material was obtained by using the accelerated chloride migration test (ACMT) and the migration coefficient was used to assess the effect of percolated ITZ. In this study, the specimen is considered as a composite material in

* Corresponding author. Tel.: +886-2-2462-2192x6406; fax: +886-2-2462-5324.
E-mail address: ccyang@mail.ntou.edu.tw (C.C. Yang).

0008-8846/$ – see front matter © 2004 Elsevier Ltd. All rights reserved.
doi:10.1016/j.cemconres.2004.05.038

which right circular cylinder aggregates with the same thickness as the specimens are embedded in a matrix of hardened cement mortar and the ITZ is around the lateral surfaces of aggregate. A model based on a regression analysis is used to determine the approximate chloride migration coefficient of percolated ITZ.

2. Experimental program

2.1. Materials and specimen preparation

Type I ordinary Portland cement, sand, and water were used as mortar matrix. The mortar proportions are summarized in Table 1; three mortars A, B, and C with w/c of 0.35, 0.45, and 0.55, respectively, and 10% by volume of Ottawa sand was used to avoid shrinkage. Marble coarse aggregates were used. Coarse aggregate was cored out from stone block with the shape of a right circular cylinder 30 mm high and with different diameters. The dimensions of various test specimens are indicated in Fig. 1a. In this study, the volume fraction of coarse aggregate (V_f, the volume of coarse aggregate/the volume of concrete) is 0.36. The total lateral surface area of the cylindrical aggregates was altered by varying the aggregate diameter and by varying the aggregate number as shown in Table 2. The aggregate cylinders were first inserted in the plastic cylindrical molds (ϕ 100 × 32 mm) and then the molds were filled with the mortar and vibrated on the vibrating table. The surface of the specimens was then smoothed, and the wet burlap was used to cover the specimens. After demolding, the specimens were cured in water (23 °C) for 6 months. After curing, the specimens were ground and polished on both top and bottom surface into 30-mm thickness before testing.

2.2. Accelerated chloride migration test

In a previous study, the ACMT was used and described in Ref. [23]. It was developed to measure the cumulative chloride ions passing through the test specimen under an applied voltage. Before the test, the cylindrical specimens (30 mm in thickness) were vacuum-saturated following the specification in ASTM C1202. A schematic presentation of the ACMT is illustrated in Fig. 2. The specimen was placed between two acrylic cells. One of the cells was filled with 0.30 N NaOH solution and the other cell with 3.0% NaCl solution. Each solution has a volume of 4500 ml in each cell. Two mesh electrodes (10 cm diameter, #20 mesh brass screen) were placed on two sides of the specimen in such a way that the electrical field is applied primarily across the test specimen. The cells were connected to a 24-V DC power source in which the NaOH electrode was the anode and the NaCl electrode was the cathode. The chloride concentration in anode cell was measured periodically using a Metrohm 792 basic ion chromatograph.

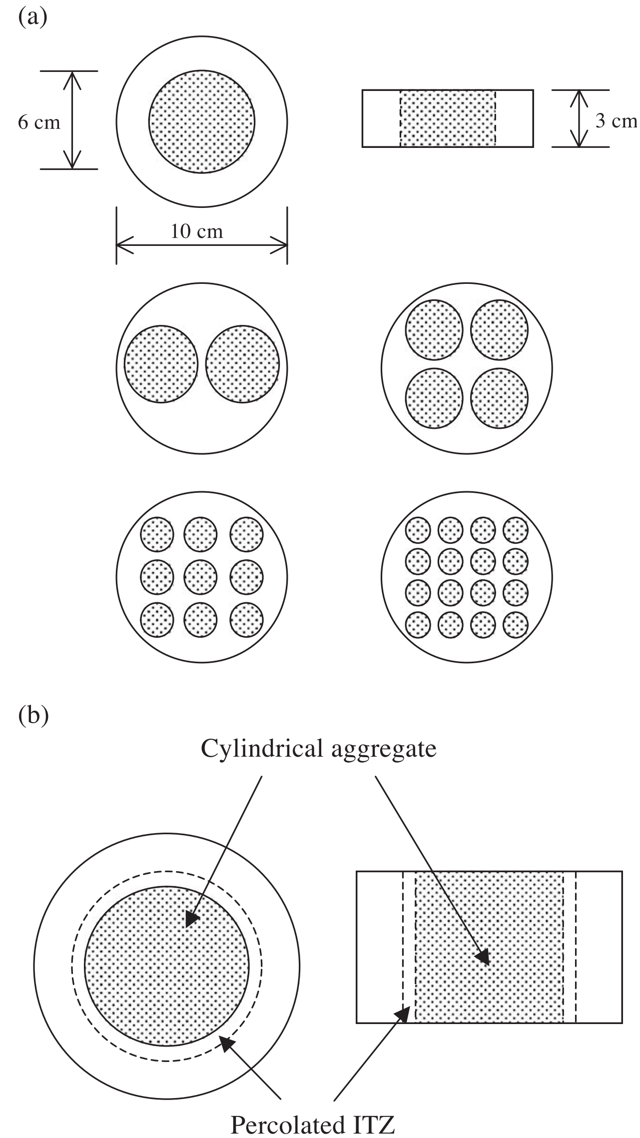

Fig. 1. Dimensions of various test specimens (a), and percolated ITZ as a layer around the cylindrical aggregate that embedded in matrix (b).

Table 1
Mix design of the mortar and w/c

Specimen type	w/c	Matrix, unit content: kg/m^3		
		Water	Cement	Fine aggregate
A00	0.35	461	1318	265
B00	0.45	516	1147	265
C00	0.55	557	1014	265

3. Results and discussion

3.1. Chloride migration coefficient

The typical result of chloride concentration in the anode solution is plotted in Fig. 3 as a function of time. Fig. 3

Table 2
The diameter, number, volume fraction, and total circumference of the cylindrical aggregates

Specimen type	Cylindrical aggregates			
	Diameter (cm)	No.	V_f	Circumference, S (cm)
A10	6	1	0.36	18.84
B10				
C10				
A15	4.243	2	0.36	26.65
B15				
C15				
A20	3	4	0.36	37.68
B20				
C20				
A30	2	9	0.36	56.52
B30				
C30				
A40	1.5	16	0.36	75.36
B40				
C40				

shows that two stages exist, nonsteady state and steady state, with respect to the change of the chloride concentration [24]. The chloride ions are in the process of migrating through the saturated pores in a specimen and have not yet reached the anode cell in the nonsteady state. In the steady state, the flux of chloride ions passing through the concrete specimen becomes constant. In order to calculate the chloride migration rate (K) for chloride ion penetration, linear regression is carried out for the steady state portion of the curve as:

$$C_{\text{cl}} = Kt + a, \tag{1}$$

where C_{cl} is the chloride concentration in anode cell, t is the elapsed time, K is the chloride migration rate, and T_s, $T_s = -a/K$, is the time span for chloride ion penetration through specimen.

In the ACMT, chloride ions are transported in a specimen under an applied voltage. Under the influence of an electrical field across the sample, the contribution of diffusion in

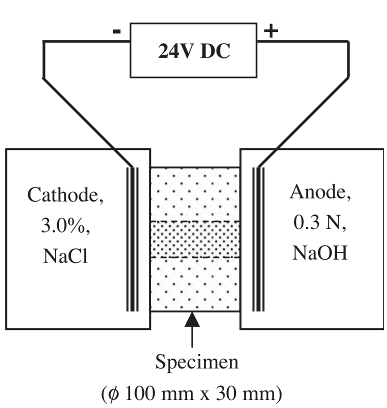

Fig. 2. Schematic diagram of ACMT.

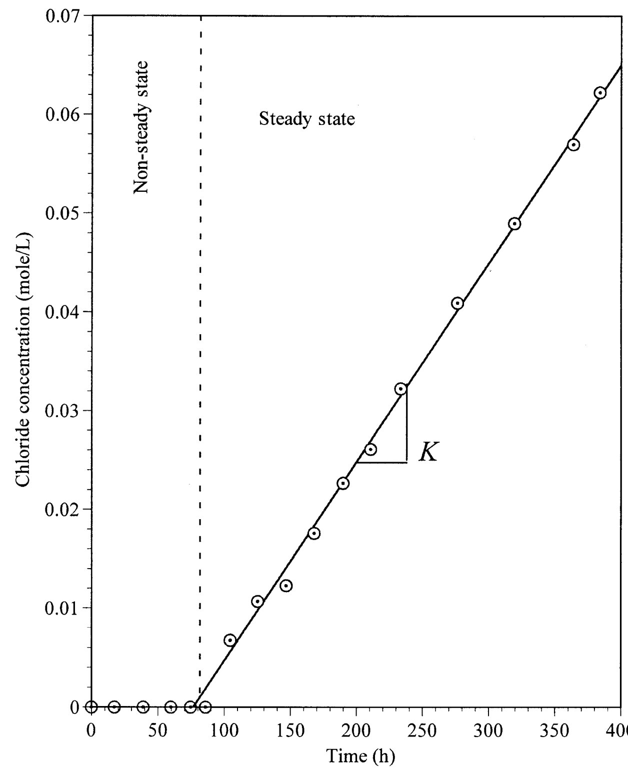

Fig. 3. Variations of chloride concentration.

concrete is small and can be neglected [25]. As the chloride flux becomes constant, the Nernst–Planck's equation that describes transport processes in solution is reduced to [25]:

$$J = -\frac{zF}{RT} M_{\text{cl}} C \frac{\partial V}{\partial x}, \tag{2}$$

where J is the constant flux of chloride in the downstream cell (mol/m^2/s), M_{cl} is the chloride migration coefficient, C is chloride concentration in the upstream cell at the cathode, V/x is the electrical field (V/m), z is the electrical charge of chloride, F is the Faraday constant (96500 C/mol), R is the universal gas constant (8.3 J/mol/K), and T is absolute temperature (K). The flux of chloride in the downstream cell is derived by calculating the migration rate according to:

$$J = \frac{V_a K}{A}, \tag{3}$$

where V_a is the volume of solution in anode cell, and A is the specimen surface exposed to chloride ions (m^2). The steady-state migration coefficient is calculated by measuring the chloride ion concentration in the anode cell, M_{cl} (m^2/s), according to:

$$M_{\text{cl}} = \frac{RT}{CF\left(\frac{V}{l}\right)} \frac{V_a K}{A}. \tag{4}$$

The chloride migration coefficients for all mixes are listed in Table 3. It appears that addition of aggregate to

Table 3
The migration coefficient and the migration coefficient on a unit volume of matrix of specimen

Specimen type	Migration coefficient, M_{cl} (1×10^{-12} m^2/s)			Migration coefficient on a unit volume of matrix (1×10^{-12} m^2/s)		
	No. 1	No. 2	Average	No. 1	No. 2	Average
A00	2.36	2.38	2.37	3.69	3.72	3.70
A10	1.52	1.54	1.53	2.38	2.41	2.39
A15	1.59	1.58	1.59	2.48	2.47	2.48
A20	1.72	1.7	1.71	2.69	2.66	2.67
A30	1.87	1.86	1.87	2.92	2.91	2.91
A40	1.97	1.92	1.95	3.08	3.00	3.04
B00	7.89	7.76	7.83	12.33	12.13	12.23
B10	5.29	5.36	5.33	8.27	8.38	8.32
B15	5.32	5.58	5.45	8.31	8.72	8.52
B20	5.75	5.82	5.79	8.98	9.09	9.04
B30	6.06	6.33	6.20	9.47	9.89	9.68
B40	6.65	6.86	6.76	10.39	10.72	10.55
C00	15.84	15.76	15.80	24.75	24.63	24.69
C10	10.84	11.22	11.03	16.94	17.53	17.23
C15	11.5	11.44	11.47	17.97	17.88	17.92
C20	12.03	12.41	12.22	18.80	19.39	19.09
C30	13.41	13.66	13.54	20.95	21.34	21.15
C40	14.81	14.18	14.50	23.14	22.16	22.65

mortar enhances the resistance of the mixture to chloride penetration.

3.2. Effect of w/c and aggregate on the chloride migration coefficient

The transport property of concrete is controlled by the transport property and content of its constituent materials. In this study, mortar is considered as matrix and the aggregate cylinders are inclusions. The aggregate used has much lower transport properties than mortar. Therefore, if the bond between aggregate and mortar is impermeable, the transport properties of the specimen will have less than that of the mortar. Shah [21] and Delagrave et al. [22] pointed out that the inclusion of aggregates in the hydrated cement past matrix has two opposite effects on the transport properties. The dilution and tortuosity effects reduce concrete permeability while the ITZ and percolation effects increase permeability. Assume that the aggregate is impermeable and a linear parallel ion flow exists. In this study, right circular cylinder aggregates with the same thickness as the specimens were used. The aggregate cylinders block the flow paths, effectively reducing the permeable area in a cross section of specimen, and need to consider the dilution effect. Since the thickness of the aggregate cylinders and specimen is the same, the length of ion flow paths may not increase and the migration coefficient in the present study was little affected by the tortuosity effect.

Considering the aggregate is relatively impermeable and a linear parallel chloride ion flow exists, a two-phase (aggregate and mortar) model for the dilution effect, the chloride migration coefficient on a unit volume of matrix, $\mathbf{M}_u$, can be expressed as:

$$\boldsymbol{M}_u = \frac{M_{cl}}{1 - V_f}. \tag{5}$$

where M_{cl} is the overall migration coefficient of specimen.

Fig. 4 shows the relationship between chloride migration coefficient on a unit volume of matrix and the w/c ratio for series 00, 10, 20, and 40. In Fig. 4, an increase of the w/c lends a significant increase of the chloride migration coefficient on a unit volume of mortar for all series. The migration coefficient is directly affected by the w/c ratio. When the lateral surface area of aggregate is fixed, the difference of chloride migration coefficient on a unit volume of matrix between mortar (series 00) and concrete increases with the w/c ratio. The chloride migration coefficients on a unit volume of matrix versus the total circumference of cylindrical aggregates are shown in Fig. 5, and the linear regression is also carried out for A, B, and C series. It is apparent that the chloride migration coefficient on a unit volume of matrix increases linearly as the total lateral surface area of aggregate increased for all series. Delagrave et al. [22] pointed out that the increase of transport property on a unit volume of matrix is attributed to the porous ITZ between the matrix and aggregate. Based on Figs. 4 and 5, the porosity increases as the w/c ratio increases, and the

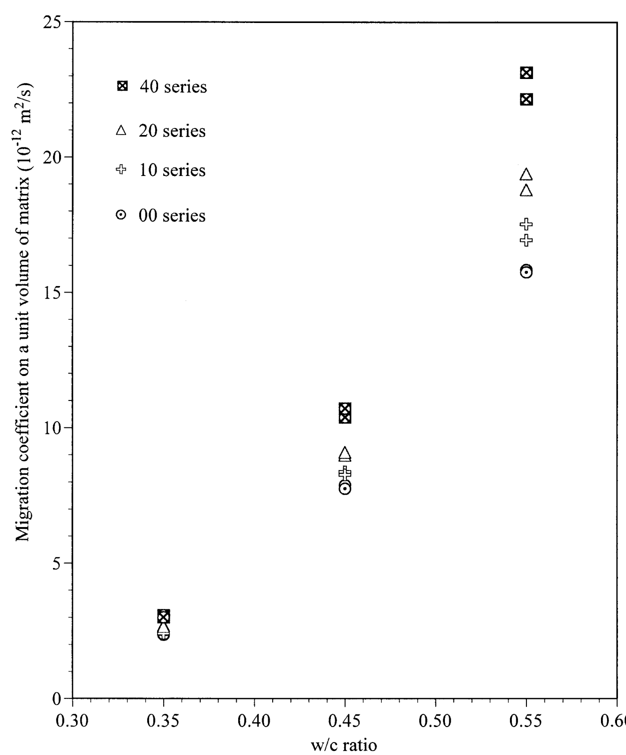

Fig. 4. The relationship between chloride migration coefficient on a unit volume of matrix and the w/c ratio for series 00, 10, 20, and 40.

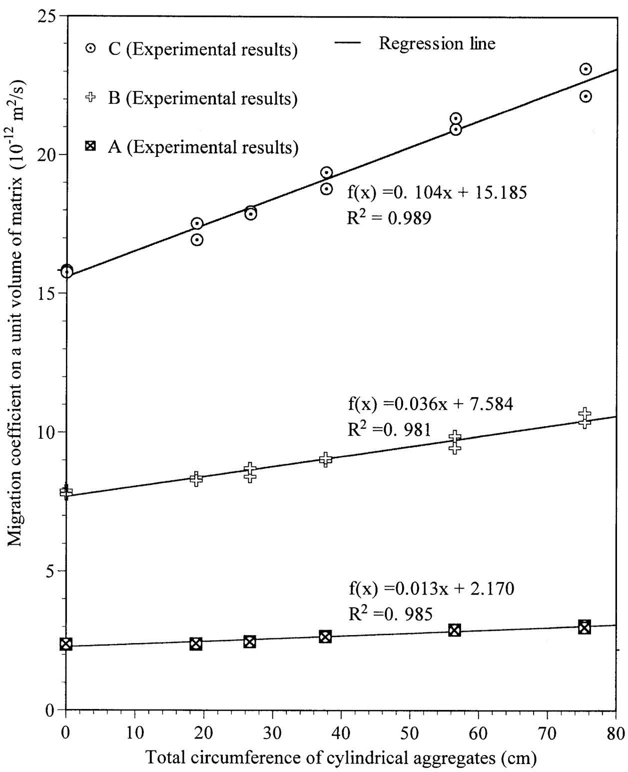

Fig. 5. The chloride migration coefficient on a unit volume of matrix versus the total circumference of cylindrical aggregates.

chloride migration coefficient is affected by the ITZ, which develops around the cylindrical aggregates. Third, the ITZ and percolation effect increases with an increase in the lateral surface area of aggregate.

3.3. Approximate migration coefficient of percolated ITZ

The thickness of the aggregate cylinders and specimen is the same, and the linear chloride ion flow is in parallel with the lateral surface of cylindrical aggregate. Therefore, the ITZ between cylindrical aggregates and matrix is percolated across the specimen. In this study, the specimen is considered as a composite material in which cylindrical aggregates are embedded in a matrix of hardened cement mortar, and the percolated ITZ is around the lateral surface of aggregates (Fig. 1b).

In this study, two cases are considered. First, the migration coefficient of the matrix is the same as that of neat mortar when the aggregate is added. Second, the migration coefficient of the matrix mortar is reduced when the aggregate is added.

3.3.1. Unaltered migration coefficient of matrix mortar

In order to investigate the approximate chloride migration coefficient of percolated ITZ, the ITZ is considered as a uniform layer around the lateral surface of aggregate cylinders and the microstructure of the matrix phase in specimen is the same as that of neat mortar (00 series). Combining the percolated ITZ effect with the dilution effect, the migration coefficient of specimen can be expressed as:

$$M_{\mathrm{cl}} = \mathbf{M}_0(1 - V_f - V_1) + \beta_u \mathbf{M}_0 V_1, \tag{6}$$

where $\mathbf{M}_0$, $\beta_u\mathbf{M}_0$, and V_1 (the volume of ITZ/the volume of specimen) are the migration coefficient of neat mortar (00 series), the migration coefficient of percolated ITZ, and the volume fraction of ITZ, respectively. This model assumes that the migration coefficient of the percolated ITZ is constant and the chloride flow in the ITZ is locally parallel to lateral surface of aggregates. In the percolated ITZ, the chloride migration coefficient of matrix ($\mathbf{M}_0$) is replaced by the chloride migration coefficient of percolated ITZ ($\beta_u\mathbf{M}_0$).

When the thickness of ITZ (h) is assumed, the volume fraction of ITZ (V_1) can be expressed as:

$$V_1 = \frac{\sum_{i=1}^{n}[\pi(r+h)_i^2 - \pi r_i^2]}{A} = \frac{\sum_{i=1}^{n}(2\pi r_i h)}{A} \cong \frac{Sh}{A} \tag{7}$$

in which A is the cross-sectional area of the specimen, r is the radius of i cylindrical aggregate, and S is the total circumference of cylindrical aggregates. From Eqs. (6) and (7), the migration coefficient of specimen is written as:

$$\frac{M_{\mathrm{cl}}}{\mathbf{M}_0} = (1 - V_f) + (\beta_u - 1)\left(\frac{Sh}{A}\right) \tag{8}$$

The measured chloride migration coefficients were normalized by the migration coefficient of the mortar with the same w/c ratio. Fig. 6 shows the relationship between normalized chloride migration coefficients of specimens and total circumference of cylindrical aggregates for different w/c, and the corresponding regression results obtained from Eq. (8) are also shown in this figure. Increasing the total circumference of cylindrical aggregates at fixed aggregate volume fraction, it certainly increases the volume fraction of ITZ. The normalized chloride migration coefficient increases as the volume fraction of ITZ increase for all series. Because it is difficult to test the ITZ separately, little information is available for the chloride migration coefficient of ITZ. Using regression analysis and that the values of β_u and h are both allowed to vary, the approximate chloride migration coefficient of percolated ITZ and the thickness of ITZ can be obtained from the Eq. (8), and the values of β_u and h are listed in Table 4. Based on the experimental and regression analytical results, the approximate percolated ITZ migration coefficient is 27.1 times of the neat mortar (00 series), and the thickness of ITZ (h) is 69 μm for the w/c ratio of 0.35. For 0.45 w/c ratio, the approximate percolated ITZ migration coefficient is 29.8 times of the neat mortar and the thickness of ITZ is 76 μm. For

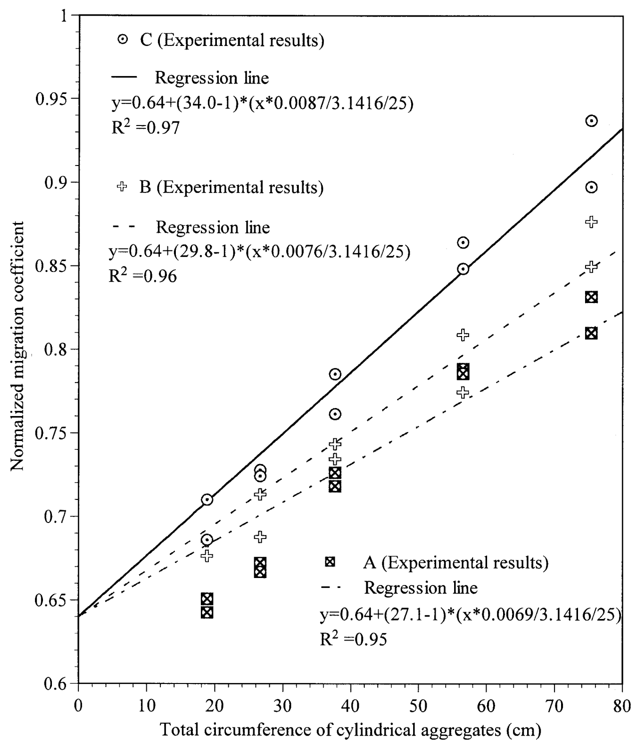

Fig. 6. The relationship between normalized chloride migration coefficient and the total circumference of cylindrical aggregates for different w/c ratio, and the corresponding regression results from Eq. (8).

0.55 w/c ratio, the approximate percolated ITZ migration coefficient is 34.0 times of the neat mortar and the thickness of ITZ is 87 μm.

3.3.2. Altered migration coefficient of matrix mortar

Several researchers [20,22] have indicated that because there is water conservation in the specimen, a higher w/c ratio in the ITZ will result in a lower w/c in the matrix mortar. The w/c ratio of the matrix mortar is reduced which tends to lower the matrix chloride migration coefficient. In order to consider this effect, a lower chloride migration coefficient in the matrix mortar, the migration coefficient of specimen, is written from Eq. (8) as:

$$\frac{M_{\mathrm{cl}}}{\mathbf{M}_0} = \alpha(1 - V_f) + \alpha(\beta - 1)\left(\frac{Sh}{A}\right) \tag{9}$$

where $\alpha\mathbf{M}_0$ is the altered migration coefficient of matrix mortar, and $\alpha\beta\mathbf{M}_0$ is the migration coefficient of percolated ITZ when aggregate is added.

Table 4
The regression results of approximate migration coefficient of percolated ITZ

Mortar type	w/c	From Eq. (8)			From Eq. (9)		
		β_u	h (μm)	R^2	α	β	R^2
A	0.35	27.1	69	.95	.92	40.6	.97
B	0.45	29.8	76	.96	.96	35.5	.97
C	0.55	34.0	87	.97	.97	37.8	.98

The measured chloride migration coefficients were normalized by the migration coefficient of the mortar with the same w/c ratio, and the normalized chloride migration coefficients are plotted in Fig. 7 as a function of total circumference of cylindrical aggregates for different w/c ratios. For computing the approximate chloride migration coefficient of percolated ITZ, the model of Eq. (9) was fitted to the experimental results to determine the altered migration coefficient of matrix mortar ($\alpha\mathbf{M}_0$) and the migration coefficient of the percolated ITZ ($\alpha\beta\mathbf{M}_0$). Using the thickness of ITZ given in Table 4, and that the parameters of α and β are allowed to vary in the regression analysis, the approximate altered migration coefficient of matrix mortar and chloride migration coefficient of percolated ITZ can be obtained from Eq. (9). The regression results are also shown in Fig. 7, and the values of α and β are list in Table 4. Based on the experimental and regression analytical results, the approximate altered migration coefficient of matrix mortar is .92, .96, and .97 times of the neat mortar (00 series) for the w/c ratio of 0.35, 0.45, and 0.55, respectively. The approximate percolated ITZ migration coefficient is 40.6, 35.5, and 37.8 times of the altered migration coefficient of matrix mortar for the w/c ratio of 0.35, 0.45, and 0.55, respectively.

In this study, two cases are considered by presence of aggregate influence chloride migration coefficient of the matrix mortar in the specimen: (1) the migration coefficient of the matrix in specimen is the same as that of neat mortar; (2) the migration coefficient of the matrix mortar is reduced.

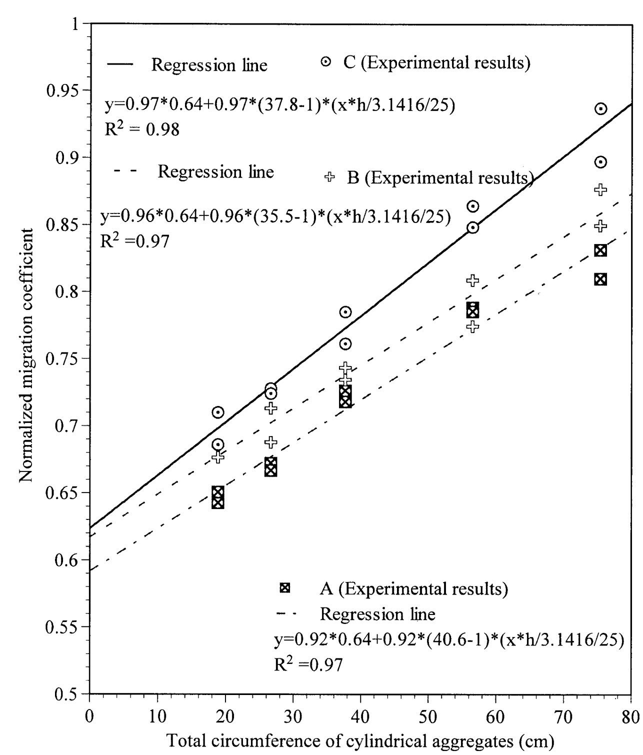

Fig. 7. The relationship between normalized chloride migration coefficient and the total circumference of cylindrical aggregates for different w/c ratio, and the corresponding regression results from Eq. (9).

Comparing the approximate percolated ITZ migration coefficient for this two cases, $\alpha\beta/\beta_u$, the ratio is 1.38, 1.14, and 1.08 for the w/c of 0.35, 0.45, and 0.55, respectively.

4. Conclusions

The chloride migration coefficient of cement-based materials is influenced by the microstructure of matrix, volume fraction of aggregate, the microstructure of ITZ, and the volume fraction of ITZ. In this study, the effect of aggregate surface area on the chloride migration coefficient of percolated ITZ was studied. Based on the results obtained from the present experimental investigation, the following conclusions can be drawn.

(1) The chloride migration coefficient is affected by the percolated ITZ, which develops between the cylindrical aggregates and matrix. The percolated ITZ effect increases with an increase in the w/c ratio.
(2) The volume of ITZ depends on the total aggregate surface and the interface thickness. The percolated ITZ effect increases with an increase in the lateral surface area of aggregate.
(3) If the migration coefficient of the matrix in specimen is assumed the same as that of neat mortar when the aggregate is added, based on the experimental and regression analytical results, the approximate percolated ITZ migration coefficient is 27.1, 29.8, and 34.0 times of the neat mortar (00 series) for w/c of 0.35, 0.45, and 0.55, respectively.
(4) If the migration coefficient of the matrix mortar is reduced when the aggregate is added, the approximate altered migration coefficient of matrix mortar is .92, .96, and .97 times of the neat mortar for the w/c ratio of 0.35, 0.45, and 0.55, respectively. The approximate percolated ITZ migration coefficient is 40.6, 35.5, and 37.8 times of the altered migration coefficient of matrix mortar for the w/c ratio of 0.35, 0.45, and 0.55, respectively.

Acknowledgements

The financial support of National Science Council, ROC, under the grants NSC 92-2211-E-019-016 and NSC 92-2211-E-157-003 is gratefully appreciated.

References

[1] P.C. Aitcin, P.K. Mehta, Effect of coarse aggregate characteristics on mechanical properties of high-strength concrete, ACI Mater. J. 87 (2) (1990) 103–107.
[2] D. Breton, A. Carles-Gibergues, G. Ballivy, J. Grandet, Contribution to the formation mechanism of the transition zone between rock–cement paste, Cem. Concr. Res. 23 (2) (1993) 335–346.
[3] D. Bonen, Calcium hydroxide deposition in the near interfacial zone in plain concrete, J. Am. Ceram. Soc. 77 (1) (1994) 193–196.
[4] D. Bonen, Calcium hydroxide deposition in the near interfacial zone in plain concrete, J. Am. Ceram. Soc. 77 (1) (1994) 193–196.
[5] K.L. Scrivener, K.M. Nemati, Percolation of pore space in the cement paste/aggregate interfacial zone of concrete, Cem. Concr. Res. 26 (1) (1996) 35–40.
[6] K.L. Scrivener, E.M. Gartner, Microstructure gradients in cement paste around aggregate particles, in: S. Midess, S.P. Shah (Eds.), Bonding in Cementitious Composites, Materials Research Society, Warrendale, 1988, pp. 77–85.
[7] R.J. Detwller, P.J.M. Monteiro, H.R. Wenk, Z. Zhong, Texture of calcium hydroxide near the cement aggregate interface, Cem. Concr. Res. 18 (5) (1988) 823–829.
[8] S. Diamond, S. Mindess, SEM investigations of fracture surfaces using stereo pairs: I. Fracture surfaces of rock and of cement paste, Cem. Concr. Res. 22 (1) (1992) 67–78.
[9] S. Diamond, S. Mindess, SEM investigations of fracture surfaces using stereo pairs: II. Fracture surfaces of rock–cement paste composite specimens, Cem. Concr. Res. 22 (4) (1992) 678–688.
[10] S. Diamond, S. Mindess, SEM investigations of fracture surfaces using stereo pairs: III. Fracture surfaces of mortars, Cem. Concr. Res. 24 (6) (1994) 1140–1152.
[11] K.L. Scrivener, A. Bentur, P.L. Pratt, Quantitative characterization of the transition zone in high strength concretes, Adv. Cem. Res. 1 (4) (1988) 230–237.
[12] T. Sugama, N. Carciello, L.E. Kukacka, G. Gray, Interface between zinc phosphate-deposited steel fibres and cement paste, J. Mater. Sci. 27 (1992) 2863–2872.
[13] P. Raivio, L. Sarvaranta, Microstructure of fiber mortar composites under fire impact effect of polypropylene and polyacrylonitrile fibers, Cem. Concr. Res. 24 (5) (1994) 896–906.
[14] A. Goldman, A. Bentur, Effects of pozzolanic and non-reactive microfillers on the transition zone in high strength concretes, in: J.C. Maso (Ed.), Interfaces in Cementitious Composites, E & FN Spon, London, 1992, pp. 53–61.
[15] D.N. Winslow, M.D. Cohen, D.P. Bentz, K.A. Snyder, E.J. Garboczi, Percolation and pore structure in mortars and concrete, Cem. Concr. Res. 24 (1) (1994) 25–37.
[16] B. Bourdette, E. Ringot, J.P. Ollivier, Modelling of the transition zone porosity, Cem. Concr. Res. 25 (4) (1995) 741–751.
[17] C.C. Yang, J.K. Su, Approximate migration coefficient of interfacial transition zone and the effect of aggregate content on the migration coefficient of mortar, Cem. Concr. Res. 32 (4) (2002) 1559–1565.
[18] E.J. Garboczi, D.P. Bentz, Digital simulation of the aggregate-cement paste interfacial zone in concrete, J. Mater. Res. 6 (1) (1991) 196–201.
[19] E.J. Garboczi, Computational materials science of cement-based materials, Mater. Struct. 26 (158) (1993) 191–195.
[20] J.D. Shane, T.O. Mason, H.M. Jennings, E.J. Garboczi, D.P. Bentz, Effect of the interfacial transition zone on the conductivity of Portland cement mortars, J. Am. Ceram. Soc. 83 (5) (2000) 1137–1144.
[21] S.P. Shah, High performance concrete: past, present and future, in: C.K.Y. Leung, Z. Li, J.T. Ding (Eds.), High Performance Concrete-Workability, Strength and Durability, Hong Kong University of Science and Technology, Hong Kong, 2000, pp. 3–29.
[22] A. Delagrave, J.P. Bigas, J.P. Olivier, J. Marchand, M. Pigeon, Influence of the interfacial zone on the chloride diffusivity of mortars, Adv. Cem. Based Mater. 5 (3–4) (1997) 86–92.
[23] C.C. Yang, S.W. Cho, R. Huang, The relationship between charge passed and the chloride–ion concentration in concrete using steady-state chloride migration test, Cem. Concr. Res. 32 (2) (2002) 45–50.
[24] M. Castellote, C. Andrade, C. Alonso, Measurement of the steady and non-steady-state chloride diffusion coefficients in a migration test by means of monitoring the conductivity in the analyte chamber comparison with natural diffusion tests, Cem. Concr. Res. 31 (10) (2001) 1411–1420.
[25] C. Andrade, Calculation of chloride diffusion coefficients in concrete from ionic migration measurements, Cem. Concr. Res. 23 (3) (1993) 724–742.